

A Newly Discovered TSHR Variant (L665F) Associated With Nonautoimmune Hyperthyroidism in an Austrian Family Induces Constitutive TSHR Activation by Steric Repulsion Between TM1 and TM7

Holger Jaeschke,* Joerg Schaarschmidt,* Markus Eszlinger, Sandra Huth, Rudolf Puttinger, Olaf Rittinger, Jens Meiler, and Ralf Paschke

Department of Internal Medicine, Endocrinology, and Nephrology (H.J., J.S., M.E., S.H., R.Pa.), University of Leipzig, 04103 Leipzig, Germany; Department of Pediatrics (R.Pu., O.R.), University Hospital Salzburg, 5020 Salzburg, Austria; and Center for Structural Biology (J.M.), Vanderbilt University, Nashville, Tennessee 37232

Objective: New in vivo mutations in G protein-coupled receptors open opportunities for insights into the mechanism of receptor activation. Here we describe the molecular mechanism of constitutive TSH receptor (TSHR) activation in an Austrian family with three generations of familial nonautoimmune hyperthyroidism.

Patients: The index patient was diagnosed with hyperthyroidism during her first pregnancy. Her first two children were diagnosed with hyperthyroidism at the age of 11 and 10 years, respectively. TSH suppression was also observed in the third child at the age of 8 years, who has normal free T₄ levels until now. TSH suppression in infancy was observed in the fourth child. The mother of the index patient was diagnosed with toxic multinodular goiter at the age of 36 years.

Methods: DNA was extracted from blood samples from the index patient, her mother, and her four children. Screening for TSHR mutations was performed by high-resolution melting assays and subsequent sequencing. Elucidation of the underlying mechanism of TSHR activation was carried out by generation and structural analysis of TSHR transmembrane homology models and verification of model predictions by functional characterization of receptor mutations.

Results and Conclusions: A newly discovered TSHR mutation L665F in transmembrane helix 7 of the receptor was detected in six members of this family. Functional characterization of L665F revealed constitutive activation for the G_s pathway and thus represents the molecular cause for hyperthyroidism in this family. The constitutive activation is possibly linked to a steric clash introduced by the L665F mutation between transmembrane helices 1 and 7. (*J Clin Endocrinol Metab* 99: E2051–E2059, 2014)

TSH/TSH receptor (TSHR) signaling controls nearly every metabolic function in thyroid cells (1). After binding of TSH, the TSHR activates the G_s protein leading to an increase of intracellular cAMP in thyrocytes. As a direct result, thyroid follicular cells grow and release thyroid hormones (1). At a higher TSH concentration, the receptor

initiates the release of G_q, which subsequently leads to iodination and thyroid hormone synthesis (1–3).

Gain-of-function mutations in the *TSHR* gene are the major molecular cause for nonautoimmune hyperthyroidism (3). Gain-of-function mutations can be either somatic or germline. Somatic mutations are found in 60%–70% of

ISSN Print 0021-972X ISSN Online 1945-7197
Printed in U.S.A.

Copyright © 2014 by the Endocrine Society
Received February 13, 2014. Accepted June 9, 2014.
First Published Online June 20, 2014

* H.J. and J.S. contributed equally to this work.

Abbreviations: CAM, constitutively activating mutation; FACS, fluorescence-activated cell sorter; FNAH, familial nonautoimmune hyperthyroidism; fT₃, free T₃; fT₄, free T₄; HRM, high-resolution melting; hTSHR, human TSHR; IP, inositol phosphate; LRA, linear regression analysis; PDB, Protein Data Bank; rh, recombinant human; TM, transmembrane helix; TSHR, TSH receptor; wt, wild type.

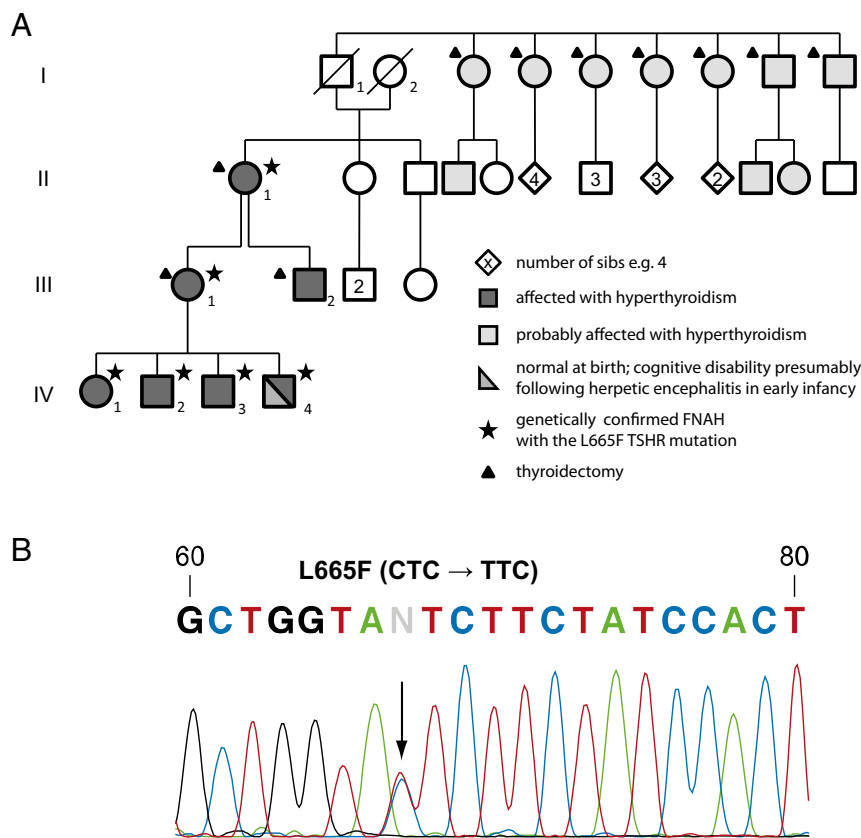


Figure 1. A, Pedigree of the Austrian family over four generations (I–IV). B, Result of one representative sequencing result for the Austrian family. All mutation-positive family members have the same substitution (C to T) at 2149, which leads to an amino acid exchange (leucine to phenylalanine) at position 665 in the TSHR.

hot thyroid nodules (4, 5). They lead to clonal expansion of the affected thyroid cell (6). The rare forms of sporadic nonautoimmune hyperthyroidism (16 published cases) or familial nonautoimmune hyperthyroidism (FNAH; 28 published cases) are mediated by germline mutations of the *TSHR* gene (7) (www.tsh-receptor-mutation-database.org). In families with FNAH the manifestation of hyperthyroidism can vary from 18 months to 74 years (8, 9). There is no relationship between the extent of basal TSHR activity and the clinical course of hyperthyroidism (10). However, the functional *in vitro* characterization of constitutively activating mutations (CAMs) found *in vivo* is a useful tool to understand the TSHR structure, function, and activation process (11). This approach has also been applied to other G protein-coupled receptors for which mutations have been detected in different diseases (12, 13).

CAMs cause a shift of the equilibrium from the inactive to an activated conformation typically induced and stabilized by binding of the endogenous ligand. Depending on the nature of the perturbation in the equilibrium, varying degrees of basal activity are observed for different CAMs. The extent of the basal activity of CAMs is an important functional readout, which can help to identify

structural features such as residue interactions necessary for a proper receptor function (14–18). Yet not only the identification and characterization of specific CAMs but also information about shared mechanisms and links of the respective constitutively activating mutation with other CAMs can therefore be crucial for understanding the mechanism of activation of the TSHR and related receptors.

Patients, Materials, and Methods

Patient

The index patient (III.1; see Figure 1A) was diagnosed with hyperthyroidism [increased free T_4 (fT₄) and free T_3 (fT₃) and suppressed TSH at presentation] with undetectable TPO and TSHR antibodies aged 18 years during her first pregnancy. After 2 years of treatment with thiamazole, her fT₄ increased to greater than 40.94 pmol/L. Therefore, she underwent thyroid surgery at the age of 22 years. Her mother (II,1) was also treated for several years for hyperthyroidism (increased fT₄ and fT₃ and suppressed TSH at presentation) and eventually underwent surgery at the age of 36 years. Similarly, thyroid surgery was also performed in the half-brother (III,2) for toxic nodular goiter at the age of 15 years (increased fT₄ and fT₃ and suppressed TSH at presentation) after relapse of hyperthyroidism during antithyroid treatment. The maternal grandfather died of cardiac failure; thyroid disease was not reported and no thyroid hormone determinations are available. All seven siblings of the grandfather (I.1) underwent surgery for nodular goiter; unfortunately, records of laboratory results are no longer available to confirm the likely hyperthyroidism for these seven siblings. Only a partial family history (but no medical records) could be obtained for some of the descendants of these seven siblings. At least three offspring of these siblings underwent thyroidectomy. No thyroid disorder or treatment was noticed in the mother of II.1.

The index patient (III.1) gave birth to four children. Of these, the older ones (IV.1,2) were diagnosed with hyperthyroidism and slightly enlarged thyroids at 10 and 11 years, respectively. Thiamazol therapy led to normal fT₄

levels. TSH suppression was also found in the third child at the age of 8 years (IV.3). He still shows normal fT_4 levels and has not yet received antithyroid treatment. The youngest boy (IV.4) exhibited TSH suppression (TSH < 0.01 mU/L, fT_4 with 1.37 ng/dL still normal) already at 6 months and was started on thiamazol because of hyperthyroidism at the age of 2 years. Sadly, his development is impaired due to being affected by epileptic encephalopathy after a herpes simplex stomatitis in infancy (before the onset of hyperthyroidism). Currently all thiamazol-treated children show normal fT_4 and fT_3 values during the antithyroid drug treatment for 3 (IV.1), 2 (IV.2), 1 (IV.3), and 1.5 (IV.4) years. A follow-up of their available TSH values during their ongoing antithyroid drug treatment is summarized in Supplemental Table 1 and the most recent thyroid parameters in Supplemental Table 2. Unfortunately, the father of these children was not available for a medical history or for laboratory results.

Nucleic acid isolation and detection of point mutations by high-resolution melting (HRM) peak analysis

Genomic DNA was extracted from peripheral blood leukocytes (QIAGEN blood kit, QIAGEN) obtained from the index patient (mother), her four children, and her mother. The screening for TSHR mutations in exons 9 and 10 was performed by real-time PCR and HRM peak analysis, using the primers shown in Supplemental Table 3 and the LightCycler 480 high-resolution melting master chemistry (Roche) on a LightCycler 480 (Roche). PCRs to detect TSHR point mutations were processed through an initial denaturation at 95°C for 10 minutes followed by 55 cycles of a three-step PCR, including 3 seconds of denaturation at 95°C, a 10-second annealing phase at 56°C, and an elongation phase at 72°C for 10 seconds. Hereafter a HRM curve was assessed from 75°C to 95°C with an increase of 0.02°C/sec and 25 acquisitions per degree.

DNAs from patient specimens known to carry a TSHR point mutation were used as positive controls in each analysis. Samples tested positive were subsequently sequenced using Big Dye-terminator chemistry (Applied Biosystems) according to the manufacturer's instructions and analyzed on an automatic sequencer ABI 3100 (Applied Biosystems).

Site-directed mutagenesis

cDNA for human *TSHR* (*hTSHR*) was inserted into the pcDNA3.1(-)/hygromycin vector using restriction sites *Xho*I and *Bam*HI. Mutations were introduced into *hTSHR*-pcDNA3.1 via site-directed mutagenesis, as described previously (19), using specifically designed primers. Mutated *TSHR* sequences were verified by Big Dye-terminator chemistry (Applied Biosystems) according to

the manufacturer's instructions and analyzed on an automatic sequencer ABI 3100 (Applied Biosystems).

Cell culture and transient expression of mutant TSHR

COS-7 cells were grown in high glucose DMEM (PAA Laboratories) supplemented with 10% fetal calf serum, 10^5 U/L penicillin, and 100 mg/L streptomycin (Gibco Life Technologies) at 37°C in a humidified 5% CO₂ incubator. Cells were transiently transfected in 12-well plates (1×10^5 cells/well for COS-7) or 24-well plates (0.5×10^5 cells/well for COS-7) with 1 μ g and 0.5 μ g DNA per well, respectively, using the GeneJammer transfection reagent (Stratagene).

Fluorescence-activated cell sorter (FACS) analyses

Transfected cells were detached from the dishes with PBS containing 0.1% BSA (FACS buffer) and transferred into Falcon 2054 tubes. Cells were washed once with FACS buffer and then incubated at 4°C for 30 minutes with a 1:400 dilution of a mouse antihuman TSHR antibody (2C11, 10 mg/L; Serotec Ltd) in the same buffer. Cells were washed twice and incubated at 4°C for 30 minutes with a 1:400 dilution of an Alexa Fluor 488-labeled F(ab')₂ fragment of goat antimouse IgG (Invitrogen, Molecular Probes) in FACS buffer. Before the FACS analysis (FACScan; Becton Dickinson and Co) cells were washed twice and then fixed with 1% paraformaldehyde. Receptor expression was determined by the median fluorescence intensity. The TSHR was set at 100%, and receptor expression of the mutant was calculated according to this value. The percentage of signal positive cells corresponds to transfection efficiency, which was approximately 50%–60% of viable cells.

cAMP accumulation assay

For cAMP assays, cells were grown and transfected in 24-well plates. Forty-eight hours after transfection, cells were incubated in the absence or presence of 100 mU/mL recombinant human (rh) TSH in serum-free medium supplemented with 1 mM 3-isobutyl-1-methylxanthine (Sigma) for 1 hour. rhTSH (Thyrogen) was purchased from Genzyme (Neu-Isenheim). Reactions were terminated by aspiration of the medium. The cells were washed once with ice-cold PBS and then lysed by the addition of 0.1 N HCl. Supernatants were collected and dried. cAMP content of the cell extracts was determined using the cAMP AlphaScreen assay (PerkinElmer) according to the manufacturer's instructions.

Linear regression analyses of constitutive activity as a function of TSHR expression (slopes)

Constitutive activity is expressed as basal cAMP formation as a function of receptor expression determined by

FACS. COS-7 cells were transiently transfected in 24-well plates with increasing concentrations of wild type (wt) or mutant TSHR plasmid DNA (50, 100, 200, 300, 400, and 500 ng/well). To transfect a constant DNA amount of 500 ng empty vector plasmid DNA was added to the mutant or wt DNA. For determination of cell surface expression see *FACS analyses*. For determination of basal intracellular cAMP accumulation, see *cAMP accumulation assay*. Basal cAMP formation as a function of receptor expression was analyzed using the linear regression module of GraphPad Prism 4 for Windows.

Activation of inositol phosphate (IP) formation

Forty-eight hours after transfection of COS-7 cells in 12-well plates, cells were incubated with 2 μ Ci [myo-³H]inositol (Amersham Biosciences) for 6 hours. Thereafter cells were incubated with serum-free DMEM containing 10 mM LiCl and 100 mU/mL rhTSH for stimulation. rhTSH (Thyrogen) was purchased from Genzyme. The evaluation of the basal and rhTSH-induced increases in the intracellular IP levels was performed by anion exchange chromatography as previously described (20). The IP values were expressed as the percentage of radioactivity incorporated from [³H]IP-1 to [³H]IP-3 over the sum of radioactivity incorporated in the IPs and phosphatidylinositol.

Homology model of the TSHR

For structural examination, a homology model of the human TSHR (hTSHR) transmembrane domain was generated using Rosetta 3 (21) as described by Nguyen et al (22). Briefly, the protein sequence of the hTSHR was aligned to the structural coordinates of each of 19 distinct template structures (see Supplemental Table 4). For each template, 200 models were built reconstructing backbone coordinates in gapped regions of the alignment using the cyclic coordinate descent protocol. The lowest energy model for each template was chosen for a more extensive sampling of the conformation of extracellular loops: 1000 models were built for each template reconstructing the loop regions with the cyclic coordinate descent protocol. In all instances, the side-chain coordinates were added from a rotamer library. The 10% lowest energy structures were clustered using bcl::Cluster (23) with a cluster radius of 3.0 Å. For the final analysis, the models were evaluated based on low energy and cluster size. In addition, a contact map for the 10% lowest energy structures of each template was generated with Rosetta's contact-Map protocol with a beta carbon distance cutoff of 10 Å. Visualization and image generation was done using the PyMOL molecular graphics system (version 1.5.0.4; Schrödinger, LLC).

Statistics

Statistical analysis was carried out using the nonparametric *t* test using GraphPad Prism 4 for Windows.

Results

Mutation analysis

To confirm the hypothesis of nonautoimmune congenital hyperthyroidism in the Austrian family, we searched for TSHR mutations by HRM and subsequent sequencing using DNA extracted from the patients' blood leukocytes. A new TSHR mutation was identified in family members (IV.1–4 and III.1–2 and II.1; Figure 1A). The newly identified TSHR variant leads to a transition in position 2149 from C to T of the *TSHR* gene (Figure 1B). The mutation is heterozygous and results in a substitution of phenylalanine (TTC) for leucine (CTC) at amino acid residue 665.

Functional characterization of the new TSHR variant L665F

Functional characterization of mutation L665F revealed a cell surface expression comparable with the wt TSHR (Figure 2A). Determination of intracellular cAMP levels confirmed the hypothesis of a constitutively activating TSHR mutation as the molecular cause of nonautoimmune congenital hyperthyroidism. Mutation L665F showed a significant increase of the ligand independent basal cAMP level of 3-fold over the basal value of the wt TSHR and a slightly higher cAMP response after administration of rhTSH compared with the wt TSHR (Figure 2B). To further validate the constitutive activity of TSHR variant L665F, we performed linear regression analyses (LRA), which allowed us to compare the receptors basal activity independently from the cell surface expression. The data obtained by LRA further confirmed the constitutive activity of the L665F variant by a slope of 2.3 (wt TSHR set at 1) (Figure 2C). Investigation of the mutation's capability to activate the Gq pathway did not show an altered basal activity or response to rhTSH (Figure 2D).

Close proximity of TSHR positions V421 [transmembrane helix (TM) 1] and L665 (TM7)

In the best scoring homology model, L665 is near three residues within TM1 and TM2, namely V421, A471, and L475. In particular, the contact between L665 and V421 occurs with the highest frequency (93%) in the best-scoring homology models (see Supplemental Table 5). This is striking because V421 is part of a cluster of amino acids between TM1 and TM7 for which constitutively activating mutations are known (Figure 3A) (5, 16, 24–28). It has been suggested that Val421 (TM1), Leu467, and A471 (TM2) as well as Leu665 (TM7) form a hydrophobic patch, and a functional characterization of V421I showed a similar phenotype like the new variant L665F (28). We hypothesize that V421I and L665F cause constitutive activation of the TSHR via the same mechanism. In both cases substitution of the side chain with a slightly larger variant resulted in constitutive activa-

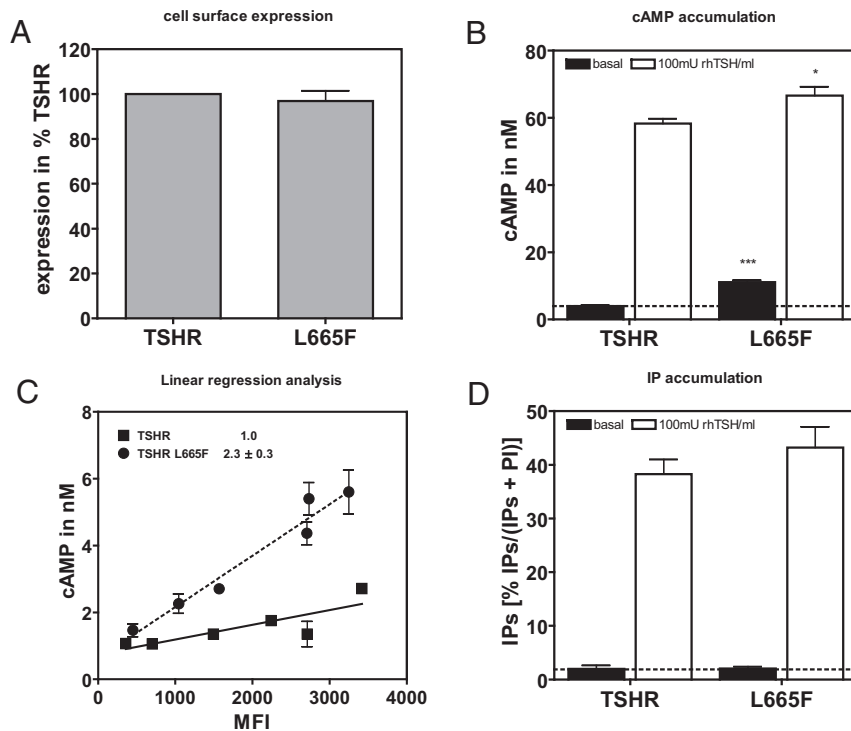


Figure 2. Functional characterization of TSHR mutation L665F. A, Cell surface expression of L665F in relation to the wt TSHR. MFI, mean fluorescence intensity. B, Intracellular basal and TSH-mediated cAMP accumulation without normalization of the expression levels. C, Determination of the constitutive activity independently from the mutation's cell surface expression by LRA. D, Basal and TSH-mediated activation of the Gq pathway. IP values were expressed as the percentage of radioactivity incorporated from [3 H]IP-1 to [3 H]IP-3 over the sum of radioactivity incorporated in IPs and phosphatidylinositol (PI). Data are presented as mean \pm SD of at least three independent experiments, each performed in duplicate. ***, $P < .001$; **, $P = .001-.01$; *, $P = .01-.05$.

tion of the TSHR, indicating that steric repulsions of the larger side chain with other parts of the protein push the receptor toward the activated conformation. The best models based on the inactive and active conformation of the A2A adenosine receptor (Protein Data Bank, PDB [<http://www.rcsb.org.pdb/>] identification: 3eml and 2ydv) support this theory by showing an increased distance between V421 and L665 in the active conformation (Figure 3B).

L665/V421 double-mutant cycle analysis

To test whether the constitutive activity of L665F is at least partially caused by steric repulsion with V421, we generated several single and double mutants. Our strategy was to replace each amino acid with a smaller amino acid (V421A and L665V) and the larger CAM (V421I and L665F). Then we created double mutants combining the four mutations. Furthermore, we tested a V421L mutant to compare the effect of steric bulk vs steric hindrance in that position. All single and double mutations were well expressed with expression levels between 84% and 99% when compared with the wt TSHR. The functional characterization of the generated constructs is summarized in Table 1.

Added steric bulk in positions L665 and V421 stabilizes the active state of TSHR

Stimulation with 100 mU/mL rhTSH resulted for some of the TSHR variants (V421I, L665F, V421I/L665F) in slightly but significantly increased cAMP levels after the administration of rhTSH (Table 1). V421I/L665F caused significantly increased, whereas V421A displays somewhat reduced ligand-induced cAMP levels. It is striking that mutation to a smaller amino acid in V421A and L665V resulted in TSHR variants exhibiting ligand-induced cAMP levels similar to or below the level of the wild-type receptor. In contrast, varying degrees of elevated cAMP levels after the rhTSH stimulation, when compared with the wt TSHR, were observed only for single or double mutants containing one or two larger amino acids, an observation consistent with the notion that added steric bulk in this region stabilizes the receptor in an active state, even after ligand binding. However, overall, these effects were small or moderate compared with the functional differences observed for the basal receptor state.

V421 and L665 form the center of a hydrophobic cluster critical for TSHR activation

The combination of the newly identified CAM L665F with the previously described CAM V421I (28) in the double-mutant V421I/L665F resulted in an increased basal cAMP activity (LRA 3.4) compared with the respective single-mutant L665F (LRA 2.3) and V421I (LRA 2.0; Table 1 and Figure 3C). Next we asked whether a mutation to a smaller amino acid in one location can compensate for mutation to a larger amino acid in the other position. This experiment tests whether the direct interaction of L665 and V421 is the only cause for constitutive activity. In this case we would expect a wt-like phenotype because the mutations should compensate each other.

The combination of the CAM V421I with L665V to V421I/L665V displayed a basal activity similar to the native TSHR (Table 1 and Figure 3C). Thus, in this scenario the substitution of the L665 side chain with the smaller V apparently compensates the V421I mutation. Furthermore, we generated the complementary exchange of V421 and L665

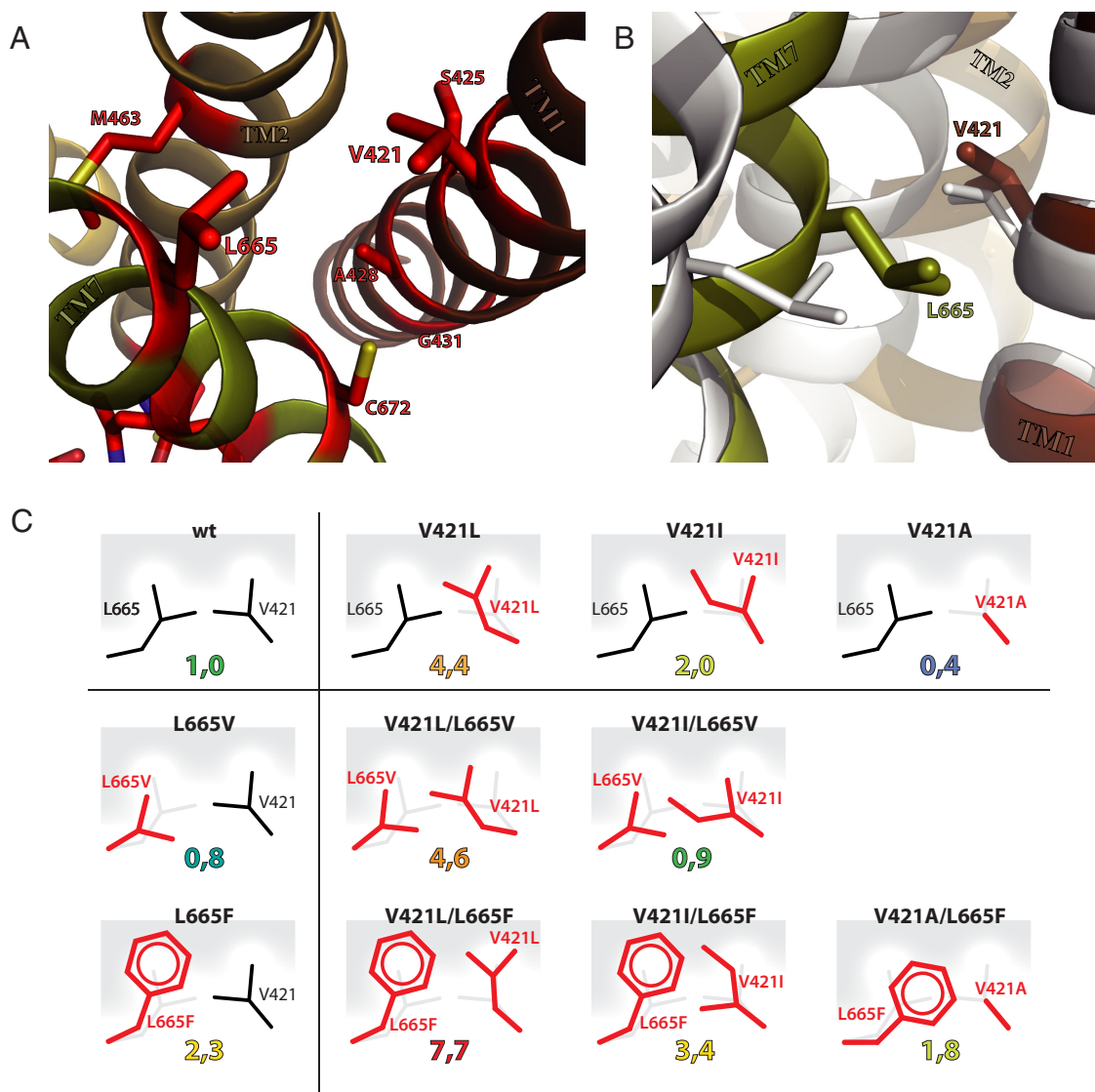


Figure 3. A, Lowest-energy homology model of the hTSHR, which is based on the crystal structure of the rat M3 muscarinic acetylcholine receptor (PDB entry 4daj). In this model, amino acid V421 is part of a cluster of residues (highlighted in red) in TM1 and TM7 for which constitutively activating mutations have been reported. B, Homology model of the hTSHR based on the crystal structure of the A2A adenosine receptor in its inactive (colored, PDB entry 3eml) and active state (white, PDB entry 2ydv) showing the side chains of L665 in TM7 and V421 in TM1. The model of the active state displays an increased distance between L665 and V421. C, Schematic representation of the generated TSHR single and double mutants and their slope determined by linear regression analyses (see also *Patients, Materials, and Methods*).

(V421L/L665V double mutant). Although the single V421L exchange resulted in an elevated basal cAMP activity (LRA 4.4) that even exceeded the basal activity of V421I, the L665V variant displayed a basal cAMP activity (LRA 0.8) similar to the native TSHR (Table 1 and Figure 3C). Here the complementary exchange V421L/L665V displayed an elevated basal cAMP activity even slightly higher than the V421L single mutant (Table 1 and Figure 3C). To test whether the substitution of V421 with a smaller amino acid could compensate the constitutive activity of the L665F mutation, we mutated V421 to an A and created the V421A/L665F double mutant. The mutation V421A resulted in decreased basal activity (LRA 0.4) of the TSHR. The combination with the CAML665F resulted in a constitutively active V421A/

L665F variant (LRA 1.8) of the receptor, yet its constitutive activity is significantly decreased in comparison with the L665F single mutant (Table 1 and Figure 3C).

Discussion

The molecular cause for nonautoimmune hyperthyroidism in an Austrian family is due to TSHR mutation L665F

The L665F mutation is a newly discovered TSHR germline mutation (www.tsh-receptor-mutation-database.org). Since the identification of TSHR mutations as molecular cause of familial nonautoimmune hyperthyroidism

Table 1. Functional Characterization of TSHR Single and Double Mutants

Construct	Localization	Cell Surface Expression	cAMP Accumulation, nM		
			Basal	100 mU/mL TSH	LRA (Slope)
TSHR	–	100	3.9 ± 0.3	52.7 ± 1.8	1
pcDNA	–	3 ± 1	1.6 ± 0.2	2.2 ± 0.3	–
V421A	TM1	93 ± 2 ^a	2.5 ± 0.1	43.8 ± 3.0	0.4 ± 0.1
V421I	TM1	96 ± 7	6.9 ± 0.5 ^b	67.3 ± 2.9 ^a	1.5 ± 0.5
V421L	TM1	89 ± 5	17.4 ± 0.6 ^b	62.8 ± 3.1	4.3 ± 0.5 ^a
L665F	TM7	97 ± 5	11.1 ± 0.6 ^b	65.2 ± 3.6 ^a	2.3 ± 0.3 ^a
L665V	TM7	99 ± 4	2.2 ± 0.1 ^b	55.8 ± 3.5	0.8 ± 0.1
V421A/L665F	TM1/TM7	99 ± 6	4.8 ± 0.2	51.8 ± 3.3	1.6 ± 0.2
V421I/L665F	TM1/TM7	92 ± 14	13.3 ± 0.5 ^c	68.7 ± 1.5 ^c	3.4 ± 0.3 ^a
V421I/L665V	TM1/TM7	98 ± 4	3.9 ± 0.5	60.4 ± 3.0	0.9 ± 0.0
V421L/L665F	TM1/TM7	88 ± 6	28.0 ± 1.3 ^b	81.3 ± 4.1 ^c	7.7 ± 0.6 ^a
V421L/L665V	TM1/TM7	84 ± 4 ^c	13.2 ± 0.1 ^b	58.0 ± 2.3	4.5 ± 0.7 ^a

COS-7 cells were transfected with plasmids harboring the nucleotide sequence of wild-type TSHR or various mutant TSHRs. The pcDNA3.1(–)/hygromycin was used as a control. Cell surface expression was quantified on a FACS flow cytometer. Basal and TSH-mediated levels of cAMP were determined after treatment of the cells with or without 100 mU/mL recombinant human TSH. Data are given as mean ± SD of at least three independent experiments (n = 3), each carried out in duplicates.

^a P = .01–.05.

^b P < .001.

^c P = .001–.01.

in 1994 after its first clinical description in 1982, 29 families with 20 different point mutations, including L665F, have been reported (25, 29). In this Austrian family, hyperthyroidism without symptoms of autoimmune thyroid disease was diagnosed in three generations. Interestingly, all four children of the third generation are carriers of the TSHR mutation, which is an unusual but not impossible event for an autosomal dominant inheritance. As previously observed in other families (8, 10), the onset of hyperthyroidism does not correlate with the extent of the ligand-independent basal activity as also shown by the different ages of onset of hyperthyroidism ranging from 2 to 11 years for the four children.

TSHR L665 is part of a cluster of hydrophobic amino acids in TM1 and TM7 for which CAMs have been reported

For some of the 61 currently known mutations that constitutively activate the TSHR *in vivo* (www.tsh-receptor-mutation-database.org), the specific molecular mechanism of receptor activation has been identified. This provided useful information regarding the activation mechanism of the TSHR (14–18). Based on predictions deduced from a homology model of the hTSHR transmembrane domain, we performed *in vitro* experiments to decipher the molecular action of the newly identified L665F mutation. Structural analysis places L665 in a cluster of amino acids in TM1 and TM7 (Figure 3A) for which CAMs have been reported. The exchange of the native L at position 665 with a larger F, as found in the Austrian

family, results in an increased basal Gs activity of the TSHR. In all reported CAMs at the TM1/7 interface, constitutive receptor activity is caused by substitutions of the initial residue by a residue with a larger side chain as shown for V421, S425, A428, G431 of TM1, and C672 of TM7 (Figure 3A) (5, 14, 24–28). This suggests that larger side chains at the respective residues push the receptor toward a ligand-independent, activated conformation. This effect also has been described for a M626I mutation (30). However, in contrast to M626I, the CAMs in TM1 and TM7 are not near the interface of the TM domain with the G protein (31).

Although the environment of L665 in the basal state of the TSHR is most likely composed of several amino acids, we focused our analysis on establishing a connection between the constitutive activity of L665F and the previously reported V421I. An increase in basal activity mediated by a larger side chain was also observed for the newly generated single mutant V421L and the double-mutants V421L/L665F and V421I/L665F. Furthermore, the effect of a longer or bulkier side chain at one position can be compensated by introducing a smaller side chain at a position in close proximity as shown for TSHR variants L665V, V421A, V421I/L665V, and V421A/L665F.

The observation that the introduction of the smaller V side chain at position L665 decreases the constitutive activity introduced by the V421I mutation as well as the reduction in constitutive activity of the V421A/L665F double mutant in comparison with the L665F single mu-

tant supports the close spatial proximity of L665 (TM7) and V421 (TM1) as suggested by the homology model of the hTSHR transmembrane domain. Comparison of the results for variants V421I and V421L showed that not only the size of the side chain affects the extent of the constitutive activity but also the stereochemistry of the introduced amino acid. The extra methyl group of the I in the V421I mutation increases the basal activity only slightly when compared with the TSHR. In contrast, the additional alteration of the center of mass of the L side chain in the V421L substitution (Figure 3C) resulted in an even higher basal receptor activity due to an increased steric repulsion with adjacent amino acids. The shifted center of mass apparently also prevents the L side chain of the V421L mutant from relocating to the space freed by the L665V mutant, resulting in an unchanged constitutive activity of the V421L/L665V double mutant in comparison with the V421L single mutant. These findings further indicate that next to the L665/V421 interaction, additional residues are involved in the constitutive activity of CAMs L665F, V421I, and V421L.

Taken together, we investigated a family with FNAH in three generations and identified the new TSHR mutation L665F as the molecular cause for this particular thyroid disorder. Furthermore, by a detailed mutagenesis study, we showed that steric repulsion between TM1 and TM7 is most likely the mechanism by which mutations L665F, V421I, and V421L as well as the previously reported CAMs at the interface of TM1 and TM7 lead to constitutive activation of the TSHR.

Acknowledgments

Address all correspondence and requests for reprints to: Professor Dr Ralf Paschke, Department of Internal Medicine, Endocrinology, and Nephrology, University of Leipzig, Liebigstrasse 20, 04103 Leipzig, Germany. E-mail: ralf.paschke@medizin.uni-leipzig.de.

This work was supported by Deutsche Krebshilfe Grant 109670.

Disclosure Summary: The authors have nothing to disclose.

References

- Vassart G, Dumont JE. The thyrotropin receptor and the regulation of thyrocyte function and growth. *Endocr Rev*. 1992;13:596–611.
- Kero J, Ahmed K, Wettschureck N, et al. Thyrocyte-specific Gq/G11 deficiency impairs thyroid function and prevents goiter development. *J Clin Invest*. 2007;117:2399–2407.
- Paschke R, Ludgate M. The thyrotropin receptor in thyroid diseases. *N Engl J Med*. 1997;337:1675–1681.
- Gozu HI, Lublinghoff J, Bircan R, Paschke R. Genetics and phenomics of inherited and sporadic non-autoimmune hyperthyroidism. *Mol Cell Endocrinol* 2010;322(1–2):125–134.
- Trulzsch B, Krohn K, Wonerow P, et al. Detection of thyroid-stimulating hormone receptor and G (s) α mutations in 75 toxic thyroid nodules by denaturing gradient gel electrophoresis. *J Mol Med* 2001; 78:684–691.
- Krohn K, Paschke R. Clinical review 133: progress in understanding the etiology of thyroid autonomy. *J Clin Endocrinol Metab*. 2001; 86:3336–3345.
- Lublinghoff J, Nebel IT, Huth S, et al. The Leipzig thyrotropin receptor mutation database: update 2012. *Eur Thyroid J*. 2012;1: 209–210.
- Schaarschmidt J, Paschke S, Ozerden M, et al. Late manifestation of subclinical hyperthyroidism after goitrogenesis in an index patient with a N670S TSH receptor germline mutation masquerading as TSH receptor antibody negative Graves' disease. *Horm Metab Res*. 2012;44:962–965.
- Gozu HI, Mueller S, Bircan R, et al. A new silent germline mutation of the TSH receptor: coexpression in a hyperthyroid family member with a second activating somatic mutation. *Thyroid*. 2008;18:499–508.
- Lublinghoff J, Mueller S, Sontheimer J, Paschke R. Lack of consistent association of thyrotropin receptor mutations in vitro activity with the clinical course of patients with sporadic non-autoimmune hyperthyroidism. *J Endocrinol Invest*. 2010;33:228–233.
- Wonerow P, Neumann S, Gudermann T, Paschke R. Thyrotropin receptor mutations as a tool to understand thyrotropin receptor action. *J Mol Med*. 2001;79:707–721.
- Smit MJ, Vischer HF, Bakker RA, Jongejan A, Timmerman H, Pardo L, Leurs R. Pharmacogenomic and structural analysis of constitutive G protein-coupled receptor activity. *Annu Rev Pharmacol Toxicol*. 2007;47:53–87.
- Schoneberg T, Schulz A, Biebermann H, Hermsdorf T, Rompler H, Sangkuhl K. Mutant G-protein-coupled receptors as a cause of human diseases. *Pharmacol Ther*. 2004;104:173–206.
- Jaeschke H, Kleinau G, Sontheimer J, Mueller S, Krause G, Paschke R. Preferences of transmembrane helices for cooperative amplification of G α s and G α q signaling of the thyrotropin receptor. *Cell Mol Life Sci*. 2008;65:4028–4038.
- Karges B, Krause G, Homoki J, Debatin KM, de Roux N, Karges W. TSH receptor mutation V509A causes familial hyperthyroidism by release of interhelical constraints between transmembrane helices TMH3 and TMH5. *J Endocrinol*. 2005;186:377–385.
- Kleinau G, Claus M, Jaeschke H, et al. Contacts between extracellular loop two and transmembrane helix six determine basal activity of the thyroid-stimulating hormone receptor. *J Biol Chem*. 2007; 282:518–525.
- Neumann S, Krause G, Chey S, Paschke R. A free carboxylate oxygen in the side chain of position 674 in transmembrane domain 7 is necessary for TSH receptor activation. *Mol Endocrinol*. 2001;15: 1294–1305.
- Urizar E, Claeysen S, Deupi X, et al. An activation switch in the rhodopsin family of G protein-coupled receptors: the thyrotropin receptor. *J Biol Chem*. 2005;280:17135–17141.
- Jaeschke H, Neumann S, Moore S, et al. A low molecular weight agonist signals by binding to the transmembrane domain of thyroid-stimulating hormone receptor (TSHR) and luteinizing hormone/chorionic gonadotropin receptor (LHCGR). *J Biol Chem*. 2006; 281:9841–9844.
- Berridge MJ. Rapid accumulation of inositol trisphosphate reveals that agonists hydrolyze polyphosphoinositides instead of phosphatidylinositol. *Biochem J*. 1983;212:849–858.
- Leaver-Fay A, Tyka M, Lewis SM, et al. Rosetta3: an object-oriented software suite for the simulation and design of macromolecules. *Methods Enzymol*. 2011;487:45–574.
- Nguyen ED, Norn C, Frimurer TM, Meiler J. Assessment and challenges of ligand docking into comparative models of G-protein coupled receptors. *Plos One* 2013;8(7):e67302.
- Alexander N, Woetzel N, Meiler J. Bcl-Cluster: a method for clustering biological molecules coupled with visualization in the Pymol

- Molecular Graphics System. *Computat Adv Biol Med Sci*. 2011;13:3–5.
24. **Biebermann H, Schoneberg T, Hess C, Germak J, Gudermann T, Gruters A.** The first activating TSH receptor mutation in transmembrane domain 1 identified in a family with nonautoimmune hyperthyroidism. *J Clin Endocrinol Metab*. 2001;86:4429–4433.
 25. **Duprez L, Parma J, Van Sande J, et al.** Germline mutations in the thyrotropin receptor gene cause non-autoimmune autosomal dominant hyperthyroidism. *Nat Genet*. 1994;7:396–401.
 26. **Fuhrer D, Warner J, Sequeira M, Paschke R, Gregory J, Ludgate M.** Novel TSHR germline mutation (Met463Val) masquerading as Graves' disease in a large Welsh kindred with hyperthyroidism. *Thyroid*. 2000;10:1035–1041.
 27. **Gozu HI, Bircan R, Krohn K, et al.** Similar prevalence of somatic TSH receptor and Gs α mutations in toxic thyroid nodules in geographical regions with different iodine supply in Turkey. *Eur J Endocrinol*. 2006;155:535–545.
 28. **Kleinau G, Haas AK, Neumann S, et al.** Signaling-sensitive amino acids surround the allosteric ligand binding site of the thyrotropin receptor. *FASEB J*. 2010;24:2347–2354.
 29. **Thomas JS, Leclere J, Hartemann P, et al.** Familial hyperthyroidism without evidence of autoimmunity. *Acta Endocrinol (Copenh)*. 1982;100:512–518.
 30. **Ringkananont U, Van Durme J, Montanelli L, et al.** Repulsive separation of the cytoplasmic ends of transmembrane helices 3 and 6 is linked to receptor activation in a novel thyrotropin receptor mutant (M626I). *Mol Endocrinol*. 2006;20:893–903.
 31. **Van EN, Preininger AM, Alexander N, et al.** Interaction of a G protein with an activated receptor opens the interdomain interface in the α subunit. *Proc Natl Acad Sci USA*. 2011;108:9420–9424.